Mechanochemical Sensing

Deutsche Ausgabe: DOI: 10.1002/ange.201502580
Internationale Ausgabe: DOI: 10.1002/anie.201502580

A Molecular Tuning Fork in Single-Molecule Mechanochemical Sensing**

*Shankar Mandal, Deepak Koirala, Sangeetha Selvam, Chiran Ghimire, and Hanbin Mao**

Abstract: *The separate arrangement of target recognition and signal transduction in conventional biosensors often compromises the real-time response and can introduce additional noise. To address these issues, we combined analyte recognition and signal reporting by mechanochemical coupling in a single-molecule DNA template. We incorporated a DNA hairpin as a mechanophore in the template, which, under a specific force, undergoes stochastic transitions between folded and unfolded hairpin structures (mechanoescence). Reminiscent of a tuning fork that vibrates at a fixed frequency, the device was classified as a molecular tuning fork (MTF). By monitoring the lifetime of the folded and unfolded hairpins with equal populations, we were able to differentiate between the mono- and bivalent binding modes during individual antibody-antigen binding events. We anticipate these mechanospectroscopic concepts and methods will be instrumental for the development of novel bioanalyses.*

A biosensor is an analytical device which utilizes recognition elements to report specific binding to biological targets. The sensitivity of a biosensor is determined by the signal transducer that converts recognition events into measurable physiochemical signals.[1] To improve the detection limit, signals are often enhanced by contributions from numerous molecules accumulated during various amplification processes, such as those employed in enzyme-linked immunosorbent assays (ELISA).[2] In conventional biosensors, analyte recognition and signal amplification are often decoupled spatiotemporally. Although such a design avoids crosstalk between two basic components in a biosensor, the physical separation deteriorates the temporal response of the sensor by complicating the biosensing procedures. Additionally, it introduces unwarranted noise because of the extra components used to interconnect the two sensing compartments.

To address these issues, it is beneficial to have a tight spatiotemporal coupling of the analyte recognition and signal transduction elements. This close coupling can be achieved by streamlining the chemical amplification step. To compensate for this simplification, ultrasensitive signal detection is required. Recent development in single-molecule techniques has offered such an opportunity. As a single-molecular reporter, however, the reproducibility and accuracy, as a result of the redundancy imparted by ensemble signals, are compromised. Therefore, it is important that single-molecule reporters are both accurate and robust. The widely used fluorescence-based single-molecule techniques[3] are not ideal to serve such a role since fluorophores are susceptible to photodamage when environmental background fluorescence is prevalent. In an effort to construct next-generation biosensors, we recently used mechanical force in a single-molecule template as a reporter for biosensing.[4] Similar to energy, mechanical force is a universal variable that can be used to describe phenomena ranging from microscopic electron–nucleus interactions and chemical bonds to macroscopic materials, such as tissues, organs, and engineered materials. Using a setup for optical levitation in a laser-tweezers instrument,[5] background mechanical noise can be reduced. Additionally, as molecules were not exposed to photons, thousands of mechanical cycles can be performed on a single-molecule template over a timeframe of days without compromising the mechanical properties of the template.

Based on our previous mechanochemical sensing endeavors,[4,6] herein we report how a mechanophore can indicate a mechanochemical event through a mechanoescence process, which is defined as a stochastic transition between two different conformations of a macromolecule at a specific tension. This process is similar to that of fluorescence, in which a fluorophore serves as a reporter for photochemical processes. This mechanochemical method should provide novel strategies that can be broadly applied to bioanalyses. As a proof of concept, we used a DNA hairpin as a mechanophore and the stochastic transition between folded and unfolded hairpins under a specific tension as the mechanoescence process to report biorecognition events. Previously, laser tweezers have been employed to investigate the interaction of ligands with individual macromolecules.[7] Although highly sensitive, such methods are cumbersome for biosensing as macromolecules with notable conformational changes are required to recognize specific ligands. In our simplified design, the mechanoescence of a DNA hairpin serves as a general reporting element while recognition units are placed separately on a DNA template. As a result of the similarity between the mechanoescence in the DNA hairpin and the vibration of a tuning fork, we named this device as a molecular tuning fork.

A regular tuning fork resonates at a constant pitch when actuated by external force (Figure 1 A). Analogous to the vibration of the prongs in a tuning fork, under a specific tension, a nucleic acid hairpin undergoes a rapid transition between unfolded and folded states by opening up and closing

[*] S. Mandal, D. Koirala, S. Selvam, C. Ghimire, Prof. H. Mao
Department of Chemistry and Biochemistry
Kent State University
Kent, OH 44242 (USA)
E-mail: hmao@kent.edu

[**] We would like to thank the NSF CHE-1026532 and NSF CHE-1415883 for partial financial support.

Supporting information for this article is available on the WWW under http://dx.doi.org/10.1002/anie.201502580.

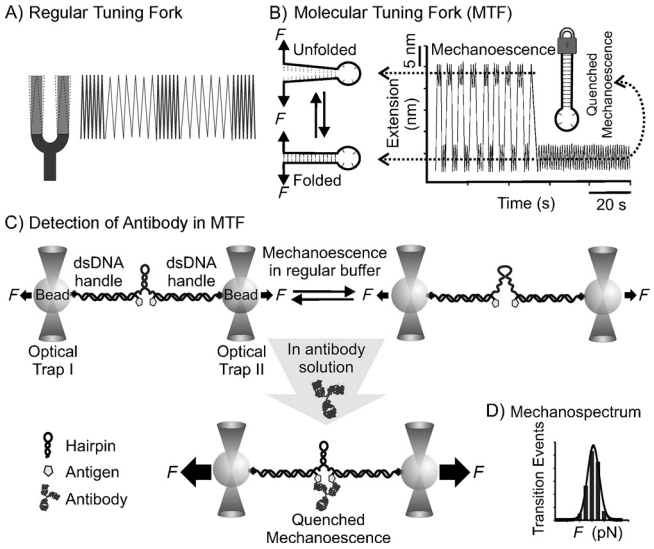

Figure 1. Schematic of the molecular tuning fork. A) A typical tuning fork with its prongs vibrating at a fixed frequency upon actuation. B) A DNA hairpin which serves as a molecular tuning fork. The hairpin undergoes random transitions between an unfolded and a folded state (mechanoescence) at a resonant force. Mechanoescence ceases outside the resonant force or when the hairpin stem is locked. C) Schematic of the molecular tuning fork for antibody detection. The hairpin is sandwiched between two dsDNA handles, which are tethered to two optically trapped beads by affinity linkages. The antigens, which specifically bind to the digoxigenin antibody, are labeled at the 3′ and 5′ ends of the dsDNA handles facing the hairpin (Figure S1). In the absence of the antibody, the hairpin mechanoesces between folded and unfolded states. Binding of the antibody quenches the mechanoescence, populating the mechanophore in the folded state. D) Mechanospectrum of a DNA hairpin mechanophore, in which the probability of the folding or unfolding transitions is plotted against mechanical excitation using force (*F*).

the two complementary strands in the hairpin stem (bi-state hopping; Figure 1 B).[8] From this perspective, the nucleic acid hairpin can be considered as a molecular tuning fork. As the frequency of a tuning fork is determined by the geometry of the fork or the property of a surrounding medium, the hairpin tuning fork can also change its transition frequencies (folding and unfolding rate constants, k_{on} and k_{off}), based on the size and composition of the hairpin as well as the buffer conditions. The hairpin can therefore report the presence of various targets that affect these on–off transitions (Figure 1 B, C). Analogous to the luminophoric or chromophoric functional groups that are responsible for the luminescence or absorbance of a molecule, we define the DNA or RNA hairpin in the molecular tuning fork device as a mechanophore,[9] and the folding and unfolding mechanochemical transitions of the hairpin as mechanoescence processes (Figure 1 C).

A mechanospectrum is generated when the likelihood of these mechanochemical transitions is evaluated over a range of mechanical forces (or mechanoexcitation; Figure 1 D). This so-called analytical mechanospectroscopy has a different focus from previous single-molecule force spectroscopy,[10] which emphasizes the effects of mechanical stress on fundamental biophysical properties, such as structures and activities, of biomacromolecules, instead of the analytical applications demonstrated herein. Similar to fluorescence spectroscopy, mechanoescence spectroscopy is expected to reveal structural, thermodynamic, and kinetic information of chemical or biochemical processes.

Unlike luminescence which suffers from irreversible photo damage and experiences significant background noise, mechanoescence has inherent advantages of high specificity and low environmental interference. First, the mechanophore is not subject to photon exposure, thereby avoiding photobleaching problems. Second, as a mechanochemical process, mechanoescence is excited by mechanical means only. These features have two consequences. On the one hand, the mechanophore is isolated from the environment by tethering to two optically levitated beads, which minimizes mechanical coupling to the environment (Figure 1 and Figure S1 in the Supporting Information). On the other hand, depending on the size and the composition of a hairpin, the mechanoescence excitation can be confined in a narrow force range, which leads to high specificity of the molecular tuning fork. Finally, as the template that hosts the mechanophore is a single molecule, it is capable of detecting individual molecules. For example, the binding of single molecules to the template can be monitored by the change in the mechanoexcitation force that leads to the maximum mechanoescence of the hairpin (see Figure 1 D and below).

Mechanospectroscopy and the molecular tuning fork are general concepts useful for many applications. As a proof of concept, herein we demonstrate that the DNA-hairpin-based MTF can function as a novel biosensor. To this end, we sandwiched a DNA hairpin between two double-stranded DNA (dsDNA) handles. The outer ends of the dsDNA handles were anchored separately to the two optically trapped beads in a laser-tweezers instrument,[11] whereas each inner end of the handles was labeled with a digoxigenin antigen (see methods and Figure S1 in the Supporting Information for the preparation of the sensing construct). The modified molecular tuning fork was placed in a microfluidic device for evaluation as a biosensor (Figure S2).

To demonstrate the MTF sensing, we first mechanically unfolded and refolded the DNA hairpin in a buffer without antibody (Figure 2 A, blue). To determine the nature of these dynamic transitions, we analyzed the change in contour length (ΔL) and the excitation force (F_{ex}) of the hairpin mechanophore with and without the digoxigenin antibody. The detected ΔL and F_{ex} values, 20.2 ± 0.2 nm and 17.3 ± 0.1 pN, respectively (Figure 3 A), for the free DNA hairpin were in agreement with expected values (see Equation S2 and Figures S3 and S4 for calculations). Upon switching the tethered DNA construct to the target channel that contains the digoxigenin antibody, different binding events were detected. Bivalent binding of the antibody to the two digoxigenin antigens flanking the hairpin is expected to quench the mechanoescence of the hairpin. Indeed, no unfolding or refolding features were detected in the force–extension (*F*–*X*) curve (Figure S5 B) at the regular excitation force ($F \approx 17.3$ pN; see Figure 2 A (blue), Figure 3 A, and Figure S5A). However at the higher F_{ex} value (40.3 ± 8.0 pN; Figure 2 A (green), and Figure 3 C (gray)), transition events were detected occasionally.

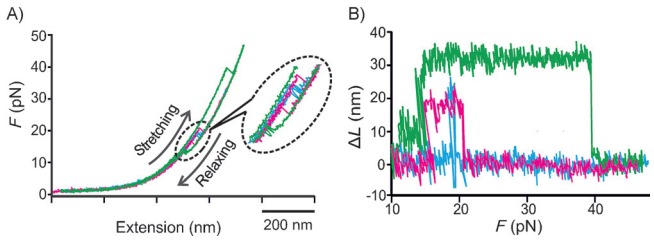

Figure 2. A) Representative force–extension (*F*–*X*) curves of the bivalent DNA construct in 10 mM Tris buffer (blue) or in a solution containing 1 nM digoxigenin antibody (green for bivalent and pink for monovalent antibody bindings). B) Change in contour length (Δ*L*) versus force (*F*) for the DNA hairpin in the absence of antibody (blue), or with bivalent (green) or monovalent (pink) antibody binding.

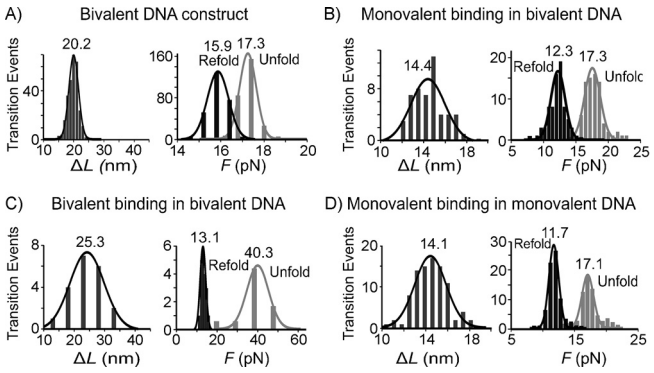

Figure 3. Mechanospectroscopy of the hairpin mechanophores. Left panels in each diagram depict Δ*L* histograms. Black and gray data in the right panels represent refolding and unfolding transitions of the hairpin, respectively. Black curves depict Gaussian fittings. A) Free bivalent DNA construct that contains two digoxigenin molecules. Bivalent DNA construct in the presence of B) monovalent or C) bivalent antibody binding. D) Monovalent DNA construct, which contains only one digoxigenin, in the presence of monovalent antibody binding.

The Δ*L* value (25.3 ± 1.7 nm; Figure 3C, left panel) of this high-force transition matched well with the calculated value (Figure S3, right panel) for the release of the nucleotides in the hairpin as well as in the single-stranded links to the dsDNA handles. Therefore, this high-force transition indicates the breaking of the bivalent antibody binding.

To evaluate whether binding of one paratope of the antibody (monovalent binding) also produces this type of rupture event, we prepared a monovalent DNA construct in which only one digoxigenin was introduced at the strand opposite to the 5′ end of the hairpin tuning fork (see the Supporting Information and Figure S4). As expected, the free monovalent DNA hairpin had transition forces almost indistinguishable from the free bivalent DNA hairpin (evident by comparison of Figure 3A to Figure S6, and also Figure S5A to Figure S5C). Upon binding with digoxigenin antibodies, although the unfolding forces remain similar between the antibody-bound monovalent hairpin (17.1 ± 0.3 pN; Figure 3D, gray) and the free bivalent construct (17.3 ± 0.1 pN; Figure 3A, gray), the refolding force of the monovalent construct (11.7 ± 0.3 pN; Figure 3D, black) was much smaller than that of the bivalent construct (15.9 ± 0.1 pN; Figure 3A, black). This introduces an obvious hysteresis between the stretching and relaxing *F*–*X* curves of the monovalent construct in the presence of the digoxigenin antibody (Figure S5D). This hysteresis is significantly smaller than that detected in the bivalent binding of the antibody to the bivalent construct (Figure 2B, green), clearly reflecting the expected difference between monovalent and bivalent antibody binding (Figure S7). Given almost identical hysteretic regions between the unfolding and refolding transitions of the hairpin (Figure S7), we concluded that monovalent antibody binding existed in the bivalent construct (Figure 2, pink).

Further analyses revealed that this monovalent binding constituted approximately 20% of the overall population in the bivalent construct (Figure S8). It is possible that malfunctioning of one digoxigenin in the template or one paratope of the polyclonal antibody may lead to monovalent binding in the bivalent construct. Currently, because of the close binding affinities and almost identical locations between the two paratopes in an IgG antibody,[12] it is rather challenging for commonly used approaches, such as surface plasmon resonance, fluorescence quenching, and ELISA, to distinguish monovalent from bivalent antibody binding. The hysteresis in the *F*–*X* curve is likely due to the steric effect of the antibody. Once a hairpin is unfolded, the sheer size of the bound IgG (150 kDa[13]) makes it more difficult to refold the hairpin kinetically, causing a decreased refolding force. These results indicate that the hairpin mechanophore can be used to report the binding of macromolecule in a remote fashion. It is interesting that the Δ*L* value for the monovalent construct (Figure S6, 15.6 ± 0.2 nm) is significantly smaller than that for the bivalent construct (Figure 3A, 20.2 ± 0.2 nm). This can be explained by the fact that the steroid structure in the digoxigenin can stack on each other.[14] As a result, the rupture event in the bivalent construct should release the nucleotides locked as a result of the stacking of the two digoxigenin molecules, leading to increased Δ*L* values (Figure S3, left panels).

Next, we monitored the antibody binding events in real time using mechanoescence of the MTF. In a microfluidic channel without the digoxigenin antibody, we maintained a constant tension ($F_{1/2}$ = 17.0 pN) in the bivalent DNA construct to facilitate the maximum mechanoescence in which the hairpin resides in the folded and unfolded states with equal probabilities (Figure 4A).

Upon binding of a digoxigenin antibody, the bivalent interaction between the antibody and the two digoxigenin ligands locks the hairpin in the folded state, quenching the mechanoescence (Figure 4B). In comparison, maximum mechanoescence was reached at $F_{1/2}$ = 17.5 pN for the monovalent hairpin that contained only one digoxigenin molecule (Figure 4C). Interestingly, when this construct was bound with a digoxigenin antibody at the same force (17.5 pN), we detected quenched mechanoescence of the hairpin tuning fork in the unfolded state (Figure 4D). To recover the maximal mechanoescence with equal populations of folded and unfolded hairpins, the $F_{1/2}$ value was reduced to 16.5 pN (Figure 4E). Analyses on the folding (k_{on}) and unfolding (k_{off}) rate constants for the hairpin tuning fork using a two-state hidden Markov model (HMM)[15] revealed decreased values with a 99% confidence level in the monovalent antibody

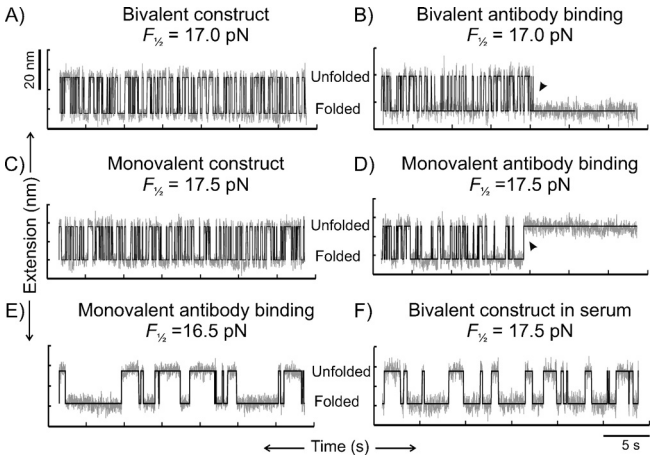

Figure 4. Real-time detection of the digoxigenin antibody by the MTF in a 10 mM Tris buffer (pH 7.4). Maximum mechanoescence of equally populated unfolded and folded states of A) a bivalent and C) a monovalent hairpin under the given forces. Binding of the digoxigenin antibody (see arrowheads) to B) the bivalent or D) the monovalent hairpin at the given force quenches the mechanoescence. E) After antibody binding in (D), the maximum mechanoescence of the monovalent hairpin at equal populations of folded and unfolded states was recovered with a reduced $F_{½}$ value (16.5 pN). F) Mechanoescence lifetime of the bivalent hairpin increases in human serum ($F_{½}$ = 17.5 pN). Gray traces depict raw data filtered with a 10 Hz bandwidth whereas black traces denote HMM fittings.

binding (Figure 4E, $k_{on} = 2.4 \pm 0.1\ s^{-1}$ and $k_{off} = 2.2 \pm 0.2\ s^{-1}$) with respect to those measured in the free hairpin (Figure 4C, $k_{on} = 3.0 \pm 0.2\ s^{-1}$ and $k_{off} = 2.9 \pm 0.3\ s^{-1}$). Corresponding to these transition kinetics, the dwell time (or lifetime) of folded and unfolded states in the monovalent antibody binding was longer (2.2 ± 1.2 s, Figure 4E) compared to the free hairpin (0.2 ± 0.1 s, Figure 4C). These observations are consistent with increased hysteresis between the unfolding and refolding events in the force-ramping experiments after monovalent antibody binding (see monovalent binding to the bivalent construct (MB) and to the monovalent construct (MM) in Figure S7). Although the monovalent binding of the antibody should not interfere as such with the mechanoescence of the hairpin, the presence of a large antibody molecule can affect the transition kinetics through either molecular crowding effects or a change in the viscosity of a microenvironment. To support this argument, we measured the mechanoescence of a free bivalent hairpin in human serum in which the presence of numerous bio-macromolecules leads to crowding effects as well as increased viscosity. Indeed, slower transition rates ($k_{on} = 2.4 \pm 0.3\ s^{-1}$ and $k_{off} = 2.5 \pm 0.2\ s^{-1}$, Figure 4F) and a longer lifetime (1.2 ± 0.7 s, Figure 4F) were obtained compared to the same construct in the diluted buffer (Figure 4A). To confirm these findings, we performed the same experiments in a Tris buffer (10 mM) with 40% bovine serum albumin (BSA; pH 7.4), which mimics molecular crowding conditions.[16] Similar results of reduced transition rates ($k_{on} = 2.4 \pm 0.2\ s^{-1}$ and $k_{off} = 2.4 \pm 0.2\ s^{-1}$, Figure S9) and longer lifetimes (3.2 ± 1.8 s, Figure S9) were obtained.

To determine the detection limit of this MTF sensing, we excited the bivalent hairpin at $F_{½} = 17.0$ pN and observed the change in the mechanoescence with and without the antibody (50 nM–10 pM) in a Tris buffer (10 mM) with 100 mM K^+ (pH 7.4). The quenching of the mechanoescence indicated the binding of the antibody.

At a concentration of 50 nM, the antibody binds to the MTF probe immediately after switching the channel, which takes approximately 15 s. The waiting time became longer with decreasing antibody concentration (see Figure 5A and Figure S10).

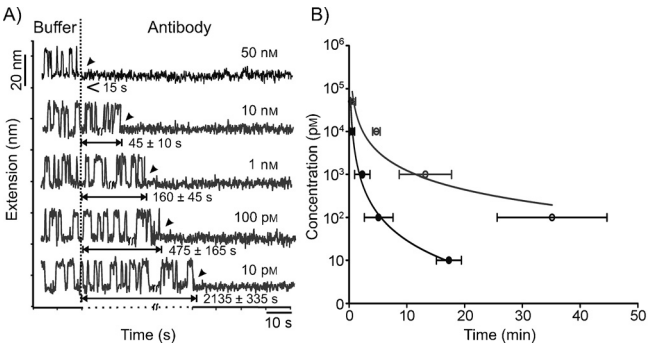

Figure 5. Detection limit of digoxigenin antibody. A) Real-time detection of the antibody in a Tris buffer (10 mM) with 100 mM K^+ (pH 7.4) by monitoring the mechanoescence of the hairpin MTF. Vertical dotted line indicates the addition of the antibody. Arrowheads indicate the bivalent binding of the antibody. B) Semilogarithmic plot of the antibody concentration versus detection time in the Tris buffer (●) or serum (○) solution using the *F–X* detection mode.

At a concentration of 10 pM, binding of the antibody was detected at 35 ± 5 min with the real-time method (Figure 5A). In comparison, only 18 ± 2 min (Figure 5B) was needed to recognize the antibody at the same concentration by measuring *F–X* curves every 20 seconds (the *F–X* mode, see the Supporting Information for details). As 30 minutes is similar to the timeframe required for PCR amplification which is used in many biosensing strategies, we set it as a threshold to determine our detection limit in Tris buffer (10 pM). With a more effective design to reduce the cross section of a microfluidic channel[4] or preconcentration techniques such as isotachophoresis,[17] we expect that the detection limit can be improved as the MTF allows single-molecule detection, the ultimate mass detection limit in molecular sensing.

To demonstrate that the MTF functions well in a clinical sample setting, we spiked digoxigenin antibody in human serum that had been centrifuged at 14000 rpm for 1 hour followed by filtration using a filter with a pore size of 200 nm. Since the mechanoescence lifetime becomes longer in the human serum for this hairpin mechanophore (Figure 4F), we evaluated the antibody binding in the *F–X* mode for 50 nM–100 pM antibody concentrations. The disappearance of the transition event at approximately 17.5 pN indicated the bivalent binding of the antibody. Such a criterion does not count for monovalent antibody binding. Therefore, the detection limit obtained by this process (100 pM within 35 min, see Figure 5B) only represents an upper limit of the sensing. As serum contains numerous macromolecules includ-

ing various antibodies, this experiment effectively established the specificity of the MTF sensing strategy.

In summary, by exploiting mechanospectroscopic methods in a DNA-hairpin-based molecular tuning fork, we have successfully demonstrated a new class of mechanochemical reporter that can recognize the binding of macromolecules. Application of this molecular tuning fork in single-molecule mechanochemical sensing leads to a system with a picomolar detection limit in approximately 30 min. Combining with the high-throughput method of magnetic tweezers,[18] we anticipated that the mechanospectroscopic approaches developed herein will have expanded applications to investigate many fundamental mechanochemical processes inside cells.

Keywords: biosensors · DNA structures · mechanochemical sensing · optical tweezers · single-molecule techniques

How to cite: *Angew. Chem. Int. Ed.* **2015**, *54*, 7607–7611
Angew. Chem. **2015**, *127*, 7717–7721

[1] a) K. Cammann, *Z. Anal. Chem.* **1977**, *287*, 1–9; b) T. Anthony, W. George, K. Isao, *Biosensors: Fundamentals and Applications*, Oxford University Press, Oxford, UK, **1987**.
[2] R. M. Lequin, *Clin. Chem.* **2005**, *51*, 2415–2418.
[3] S. Weiss, *Science* **1999**, *283*, 1676–1683.
[4] D. Koirala, Z. Yu, S. Dhakal, H. Mao, *J. Am. Chem. Soc.* **2011**, *133*, 9988–9991.
[5] a) J. R. Moffitt, Y. R. Chemla, D. Izhaky, C. Bustamante, *Proc. Natl. Acad. Sci. USA* **2006**, *103*, 9006–9011; b) J. R. Moffitt, Y. R. Chemla, S. B. Smith, C. Bustamante, *Annu. Rev. Biochem.* **2008**, *77*, 205–228.
[6] a) D. Koirala, P. Shrestha, T. Emura, K. Hidaka, S. Mandal, M. Endo, H. Sugiyama, H. Mao, *Angew. Chem. Int. Ed.* **2014**, *53*, 8137–8141; *Angew. Chem.* **2014**, *126*, 8275–8279; b) P. Shrestha, S. Mandal, H. Mao, *ChemPhysChem* **2015**, DOI: 10.1002/cphc.201500080.
[7] a) D. Koirala, S. Dhakal, B. Ashbridge, Y. Sannohe, R. Rodriguez, H. Sugiyama, S. Balasubramanian, H. Mao, *Nat. Chem.* **2011**, *3*, 782–787; b) J. Stigler, M. Rief, *Proc. Natl. Acad. Sci. USA* **2012**, *109*, 17814–17819.
[8] a) M. T. Woodside, W. M. Behnke-Parks, K. Larizadeh, K. Travers, D. Herschlag, S. M. Block, *Proc. Natl. Acad. Sci. USA* **2006**, *103*, 6190–6195; b) J. Liphardt, B. Onoa, S. B. Smith, I. Tinoco, C. Bustamante, *Science* **2001**, *292*, 733–737.
[9] P. A. May, J. S. Moore, *Chem. Soc. Rev.* **2013**, *42*, 7497–7506.
[10] a) M. Rief, F. Oesterhelt, B. Heymann, H. E. Gaub, *Science* **1997**, *275*, 1295–1297; b) C. Gosse, V. Croquette, *Biophys. J.* **2002**, *82*, 3314–3329.
[11] H. Mao, P. Luchette, *Sens. Actuators B* **2008**, *129*, 764–771.
[12] J. S. Huston, D. Levinson, M. Mudgett-Hunter, M. S. Tai, J. Novotný, M. N. Margolies, R. J. Ridge, R. E. Bruccoleri, E. Haber, R. Crea, *Proc. Natl. Acad. Sci. USA* **1988**, *85*, 5879–5883.
[13] a) P. Travers, M. Walport, M. Shlomchik, M. S. C. Janeway, *Immunobiology: The immune system in health and disease*, 5th ed., Garland Science, New York, **2001**; b) L. J. Harris, S. B. Larson, K. W. Hasel, A. McPherson, *Biochemistry* **1997**, *36*, 1581–1597.
[14] P. Roy, C. M. Roth, M. N. Margolies, M. L. Yarmush, *Mol. Immunol.* **1999**, *36*, 1149–1158.
[15] a) S. A. McKinney, C. Joo, T. Ha, *Biophys. J.* **2006**, *91*, 1941–1951; b) D. Koirala, J. A. Punnoose, P. Shrestha, H. Mao, *Angew. Chem. Int. Ed.* **2014**, *53*, 3470–3474; *Angew. Chem.* **2014**, *126*, 3538–3542.
[16] a) S. Dhakal, Y. Cui, D. Koirala, C. Ghimire, S. Kushwaha, Z. Yu, P. M. Yangyuoru, H. Mao, *Nucleic Acids Res.* **2013**, *41*, 3915–3923; b) R. J. Ellis, A. L. Minton, *Nature* **2003**, *425*, 27–28.
[17] M. Bercovici, C. M. Han, J. C. Liao, J. G. Santiago, *Proc. Natl. Acad. Sci. USA* **2012**, *109*, 11127–11132.
[18] I. De Vlaminck, T. Henighan, M. T. J. van Loenhout, I. Pfeiffer, J. Huijts, J. W. J. Kerssemakers, A. J. Katan, A. van Langen-Suurling, E. van der Drift, C. Wyman, C. Dekker, *Nano Lett.* **2011**, *11*, 5489–5493.

Received: March 19, 2015
Published online: May 8, 2015

